Journal of Thermal Analysis, Vol. 52 (1998) 773-780

ORDER PROCESSES IN Cu–Zn–Al SHAPE MEMORY ALLOYS
Quantitative approach to M_s values by resistance measurements

*A. Isalgué and V. Torra**

CIRG-DFA-ETSECCPB, UPC, Campus Nord, B-4, E-08034 Barcelona, Spain

Abstract

Analysis of the experimental results on Cu–Zn–Al shape memory alloys indicates that the transformation temperatures (for instance, M_s) fluctuate in long-term records. Continuous measurements of electrical resistance R (five significant figures) are made with controlled and programmed temperature (resolution 0.005 K). The experimental analysis suggests a partitioning of resistance into two additive contributions: phonon and order (or R^*). The time behaviour of R^* represents the dependence of M_s on time. The results indicate that the effects of time and temperature in the austenite phase can be represented by two independent differential equations: the long-time fluctuations in the transformation temperature are predictable and the uncertainty reduces to ±0.15 K.

Keywords: atomic order, martensitic transformation, modeling, shape memory, simulation, time behaviour

Introduction

The martensitic transformation between metastable phases is the origin of shape memory effects. Shape memory alloys are smart materials: they can serve simultaneous functions as sensors and actuators. The applicability of the material for on-off actions needs only a poor reliability, but the main interest in continuous actuators focuses on the coexistence domain (from 0 to 100% of the martensite phase) with a small hysteresis as in Cu-based alloys [1–2]. Reliability is a critical word in applications and the industrial interest needs completely guaranteed behaviour. Determination of predictable rules of M_s against time and temperature is a necessary tool for classification of the available materials.

Analysis of the classical experimental results after quenching indicates that the transformation temperature (for instance M_s) fluctuates randomly in long-

* Author for correspondence: e-mail: vtorra@etseccpb.upc.es

1418–2874/98/ $ 5.00

Akadémiai Kiadó, Budapest
Kluwer Academic Publishers, Dordrecht

term obsservations within relatively reduced margins ($\Delta M_s \approx \pm 2$ K). In general, the changes in M_s have been associated with many causes: atomic order (B2 and $L2_1$ in Cu–Zn–Al alloys), domains of order, elastic dipoles, dislocations (creation, movement and evolution), etc. [3–12].

In the present work, continuous measurements of electrical resistance with improved resolution (around five significant figures) are considered with a controlled and programmed temperature, the behaviour of the material in the austenite phase near room temperature (T_{RT}) is quantified. Analysis of the experimental results allows a quantitative formalism by means of two differential equations relating to two order phenomena. The phenomenological model determines the behaviour of M_s against time, including the effects of the time evolution of room temperature.

Experimental

A computer-controlled system with high resolution was used. The computer reads the temperature from a Pt-100 platinum resistance via a Hewlett Packard 3478 A digital multimeter or DMM (resolution 0.001 Ω). Temperature is controlled via the Peltier effect to a resolution and reproducibility of ±0.005 K, as described elsewhere [13]. DC current and voltage are separately acquired from two DMM (via GPIB) in order to obtain the resistance of the sample. A four-wire method with current direct and reversed (near 0.2 A) was used, due to the low values of the resistance (around 2 mΩ). Averaging of 256 double readings (positive and negative values) allows an increased resolution in resistance (0.1 μΩ), equivalent to nearly five significant figures (or 0.005%).

A single crystal of Cu–Zn–Al was used, with an electron concentration of 1.48 electrons/atom. The nominal value of M_s related to the standard composition was 273 K. Measurements started with solubilization at 1023 K and a quench process in water at room temperature. After quenching around one thou-

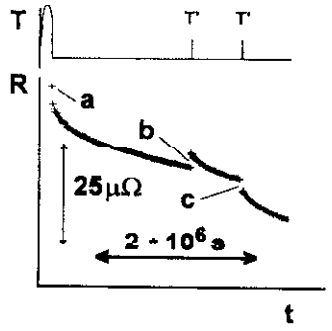

Fig. 1 Time evolution of resistance values: — temperature *vs.* time (schematic), +++ resistance after soldering (a) the electrical wires onto the sample. The resistance *vs.* time displays the action of two microheat treatments (b and c)

sand thermal cycles (austenite-martensite-austenite) were performed on the same sample, and the temperature was programmed and controlled during more than 3 years. Some perturbative temperature effects occurred during this time: the soldering of the wires produced a relevant effect (Fig. 1), and some power failures with badly controlled re-starting of the measuring system introduced supplementary effects.

Results very similar to those reported here were obtained on a Cu–Zn–Al sample with different composition (electron concentration 1.46 electrons/atom) and different initial M_s (near 303 K).

Results and discussion

Cycling from austenite to martensite and back to austenite induces a classical increase in the hysteresis width (because of the creation of dislocations), but after several hundreds of thermal cycles the effect is irrelevant (a near-saturation situation is reached). Also, cycling induces local changes in M_s relating to martensite stabilization and the coexistence of parent and martensite phases via minor effects in recoverable stabilization [14]. That effect is avoided in this work: the M_s measurements were separated by several days. Badly controlled re-starting of the system produces perturbative effects (by unexpected heating) in the form of M_s changes, and can eventually produce effects relating to structural changes: after these, the width of the hysteresis cycle increases slightly and the temperature M_s generally decreases. The action might be interpreted as a minor precipitation effect, as a result of the mixed action: achieved by temperature (T>380 K) and time (around 36 h).

After a temperature perturbation in the austenite phase, the resistance of the sample reveals an unexpected apparent time dependence. Figure 1 shows the behaviour after the soldering of wires onto the sample. Two heating effects at the

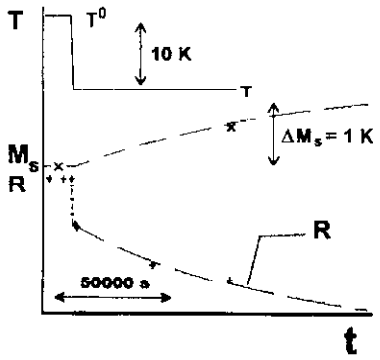

Fig. 2 Effect of a temperature step from a previous steady state; Behaviour of temperature (T), M_s and resistance (R) after a temperature step (from T^0 to T), – – – computed values; ××× or + + + experimental values

same temperature T', but with different lengths of time ($\Delta t_b << \Delta t_c$), produce different effects on the resistance evolution. Figure 1, for instance, exhibits an increase (in event *b*) and a decrease (in event *c*). After a long time at a constant temperature T°, if a temperature step is made (from T° to T in Fig. 2), the behaviour of the resistance is nearly exponential and two time constants τ_1 and τ_2 (with 'low' and 'high' values) can be determined for each actual sample temperature T. The time evolution of M_s is similar to the resistance dependence on time.

The main part of the analysis was carried out after a relevant number of cycles (transformation-retransformation) on the sample, to stabilize dislocation concentration. From series of experimental measurements (temperature step analysis from steady to steady states) the fitted temperature dependence (in K) of the time constants (in s) reads

$$\tau_1=\exp\left(-29.304+\frac{13630}{T}\right);\quad \tau_2=\exp\left(-16.933+\frac{10330}{T}\right) \tag{1}$$

where $M_s<T<390$ K. The estimated uncertainty of the time constant values is around 2%.

The activation energy values relate to the mean dislocation concentration. Cycling after quenching increases the dislocation concentration, and the time constant values also increase.

To visualize the M_s evolution for a more complex temperature *vs.* time path, a characteristic resistance R^* can be defined. From experimental values of resistance (needed resolution: greater than 0.5%), the characteristic resistance R^* relating to order effects can be calculated by subtracting the phonon contribution:

$$R^*(T)=R(T)-\alpha(T-T_{ri}) \tag{2}$$

where α is the dR/dT value estimated from fast temperature changes and T_{ri} is the reference temperature (usually in the steady state). The time behaviour of R^* is related to the M_s values *vs.* time (e.g. Figs 3 and 4). In Fig. 3, a minor effect of

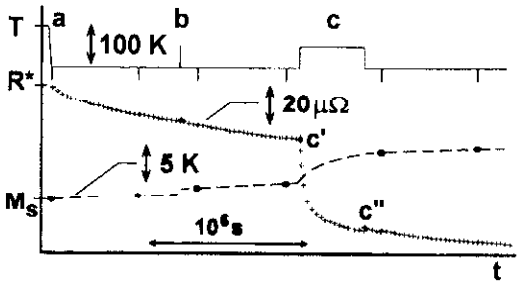

Fig. 3 Time and temperature effects on M_s; Temperature T (—, upper) reduced resistance R^* (+ + +, middle) and M_s values (• • •, bottom) *vs.* time; a) Initial micro-thermal treatment: 13 h at 405 K; b) Effect of a microheat: T goes to 363 K and returns to 298 K in 8 min; c) Aging at 363 K during 4.7 days

continuity in c' and c'' relates to second-order thermal dilatation effects on the actual resistance values. Evaluation of the explicit dependences of R^* on room temperature and time seems a way to evaluate the time parameters of an alloy and its usefulness for a guaranteed application.

Two different and independent time constants suggest the existence of two internal phenomena or, as a working hypothesis, two independent atomic order processes possibly related to the temperature dependence of the vacancy concentration. Analysis of the experimental results allows a quantitative formalism, by means of two differential equations relating to two order phenomena, which determine the behaviour of M_s against time and room temperature. In the steady state, at a rigorous constant reference temperature T_{rt}^* the transformation temperature M_s is only related to the T_{rt}^* value:

$$M_s \equiv M_s(T_{rt}^*) \tag{3}$$

In a variable-temperature situation, the two ordering phenomena are represented by two equivalent temperatures $T_1(t)$ and $T_2(t)$ tracking the actual sample temperature or 'room temperature', $T_{RT}(t)$. With the previous steady state accomplished, the start initial conditions reads

$$T_{rt}^* = T_{RT}(t=0) = T_1(t=0) = T_2(t=0) \tag{4}$$

After a temperature step, the M_s behaviour approximates to an exponential form. Unrestricted evolution of T_{RT} determines the temperature dependence of the time constants (T in Eq. (1) is now T_{RT}). The phenomenological formalism, via the equivalent temperatures, reads

$$\frac{dT_1}{dt} = -\frac{1}{\tau_1}(T_1 - T_{RT}); \quad \frac{dT_2}{dt} = -\frac{1}{\tau_2}(T_2 - T_{RT}) \tag{5}$$

On solution of the two differential equations, the time dependences of T_1 and T_2 are determined and M_s can be computed by using

$$M_s(t,T_{RT}) = M_s(t=0,T_{rt}^*) + k_1(T_1 - T_{rt}^*) + k_2(T_2 - T_{rt}^*) \tag{6}$$

Experimental measurements based on temperature-step analysis establish the k_1 and k_2 values:

$$k_1 = -0.105; k_2 = -0.067 \tag{7}$$

From a previous steady state, the fluctuations of M_s are relevant: nearly 17% of the room temperature changes. With the described formalism, the time–temperature effects on the parent phase can be simulated by using the Runge-Kutta classical algorithm [15], and the coherence between experimental and calculated values of M_s is excellent (Figs 4 and 5, where the mean scatter in M_s is 0.15 K).

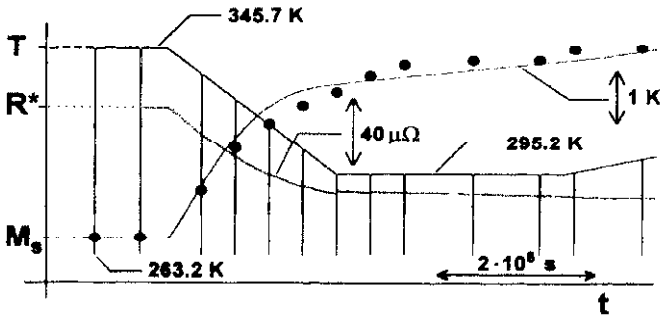

Fig. 4 Temperature and time effects; Predictable behaviour *vs.* time: T, experimental temperature; Aging: higher value 355.65 K, lower value 295.24 K; Cycles: lower value 265 K; R^*: reduced resistance defined in Eq. (5); M_s: transformation temperature: • • • measured, — computed with the parameters given in the text

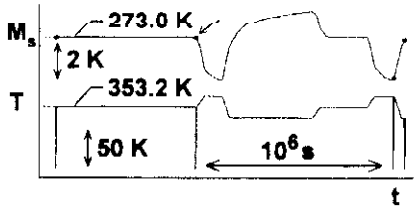

Fig. 5 Temperature and time effects after a steady state: predictable behaviour against time; M_s: calculated M_s values; T: experimental aging temperatures; full dots (•) – experimental measurements

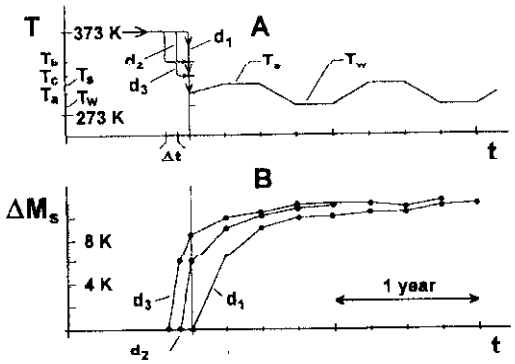

Fig. 6 Calculated effects after a classical aging at 373 K; A) Simulated path of temperature *vs.* time; Path d_1: direct quenching to a spring temperature T_a (298 K); Path d_2: step quenching to T_b (one month at 338 K) and final temperature T_a; Path d_3: two-step quenching: one month at T_b (338 K), one month at T_c (318 K) and final temperature T_a; B) Calculated values of M_s change relative to the initial value at 373 K for paths d_1, d_2 and d_3

In Fig. 5, there is a complex temperature *vs.* time path, and the computed values display good agreement with the measured M_s values obtained by avoiding perturbative effects relating to cycling and M_s measurements.

The results indicate that microheating or room temperature effects modify the M_s value. For instance, yearly effects relating to the mean temperature in summer and winter induce predetermined and particular M_s changes. With the simulation, the room temperature effects on the parent phase can be quantitatively predicted (Figs 4 and 5). In the alloys used, the classical aging at 373 K seems inappropriate and, avoiding possible precipitation effects, induces more long-lasting effects on M_s (see simulation in Fig. 6). After aging at 373 K, 2 months at intermediate temperatures (338 K and 318 K) accelerates the main evolution towards the seasonal fluctuation between winter at mean temperature T_w and summer at T_s (in Fig. 6, 283 K and 308 K, respectively). Path d_3 is highly efficient relative to the standard aging (path d_1). Computer simulation permits an evaluation of several aging processes and choice of the optimal aging minimizing the time spent for a given purpose.

Two-order processes are active in Cu–Zn–Al alloys: B2 and $L2_1$ relating to near and next-near neighboring atoms [2]. Actually, the structural analysis centers on equilibrium phases or relatively intense phenomena, e.g. the after-quenching measurements (see [16] for detection in a related alloy). An explicit link between the time constants and the B2 and $L2_1$ atomic order is uncertain at the present state of the art.

Conclusions

If resistance measurements with improved resolution are used, it is possible to quantify the behaviour of the material in the austenite phase near room temperature. The experimental analysis (resolution greater than 0.5% is needed) suggests a partition of resistance R into a phonon contribution and an order contribution R^*. The time behaviour of R^* relates, in qualitative form, to the dependence of M_s on time.

Analysis of the experimental results allows a quantitative formalism that determines the behaviour of M_s against time and room temperature effects. When two differential equations relating to two equivalent order temperatures are used, the coherence between experimental and simulated values is excellent. From the formalism, a predictable approach for a given alloy can be attained.

* * *

This research was carried out in the frame of DGICYT HF 1996-0010. V. T. acknowledges partial support from Dir. Pol. Terr. (Generality of Catalonia).

References

1 L. Delaey, 'Diffusionless Transformations,' Material Science and Technology, R. W. Cahn et al. ed., VCH, Weinheim, Germany, 5 (1991) 339.

2 M. Ahlers, Prog. Mater. Sci., 30 (1986) 135.
3 R. Rapacioli and M. Ahlers, Acta Metall., 27 (1979) 777.
4 A.Planes, J. Viñals and V. Torra, Phil. Mag., A 48 (1983) 501.
5 J. Viñals, V. Torra, A. Planes and J. L. Macqueron, Phil. Mag., A 50 (1984) 653.
6 K. Tsuchiya, D. Miyoshi, K. Tateyama, K. Takezama and K. Marukawa, Scripta Met. Mater., 31 (1994) 455.
7 T. Tadaki, 'Aging behaviour of some shape memory alloys and its origin' in Shape Memory Materials '94, Chu Youyi and Tu Hailing Eds. (International Academic Publishers, Beijing, 1994) p. 31.
8 Y. Dhazi and W. Zhongguo, 'Aging effects of Cu-based shape memory alloys' in Shape Memory Materials '94, Chu Youyi and Tu Hailing Eds. (International Academic Publishers, Beijing, 1994) p. 31.
9 T.Tadaki, Y. Nakata and K. Shimizu, J. Physique, IV 5 (1995) C8 81.
10 Y. Murakami, Y. Nakajima and K. Otsuka, Scripta Materialia, 34 (1996) 955.
11 L. Buffard, 'Influence des interactions, des défauts, de l'ordre-désordre et de la transformation martensitique sur l'hystérésis mécanique de l'alliage à mémoire de forme Cu–Zn–Al–Ni' Ph D (1991) Ecole Centrale de Lyon, France (in French).
12 A. Isalgue, F. C. Lovey, J. L. Pelegrina and V. Torra, J. Phys. IV Coll. C8 5 (1995) C8-853.
13 A. Amengual, A. Isalgue, F. C. Lovey, F. Marco and V. Torra, J. Thermal Anal., 38 (1992) 593.
14 J. L. Pelegrina, M. Rodriguez de Rivera, V. Torra and F. C. Lovey, Acta Metall. Mater., 43 (1995) 993.
15 W.H. Press, S. A. Teukolsky, W. T. Vetterling and B. P. Flanner, Numerical Recipes in FORTRAN (Cambridge University Press, Cambridge, U. K., 1992) p. 704.
16 X. Ren and K. Otsuka, Nature, 389 (1997) 579.